REPORT DOCUMENTATION PAGE

Form Approved
OMB No. 0704-0188

1. REPORT DATE *(DD-MM-YYYY)*	**2. REPORT TYPE**	**3. DATES COVERED** *(From - To)*
15 May 2016	Conference Paper	18 Mar 2016 – 15 May 2016

4. TITLE AND SUBTITLE
Acoustically Forced Coaxial Hydrogen / Liquid Oxygen Jet Flames

5a. CONTRACT NUMBER

5b. GRANT NUMBER

5c. PROGRAM ELEMENT NUMBER

6. AUTHOR(S)
Mario Roa, David Forliti, Al Badakhsahn, Doug Talley

5d. PROJECT NUMBER

5e. TASK NUMBER

5f. WORK UNIT NUMBER
Q0YA

7. PERFORMING ORGANIZATION NAME(S) AND ADDRESS(ES) AND ADDRESS(ES)

Air Force Research Laboratory (AFMC)
AFRL/RQRC
10 E. Saturn Blvd.
Edwards AFB, CA 93524-7680

8. PERFORMING ORGANIZATION REPORT NO.

9. SPONSORING / MONITORING AGENCY NAME(S) AND ADDRESS(ES)

Air Force Research Laboratory (AFMC)
AFRL/RQR
5 Pollux Drive
Edwards AFB, CA 93524-7048

10. SPONSOR/MONITOR'S ACRONYM(S)

11. SPONSOR/MONITOR'S REPORT NUMBER(S)
AFRL-RQ-ED-TP-2016-069

12. DISTRIBUTION / AVAILABILITY STATEMENT
Approved for public Release; Distribution Unlimited. PA Clearance Number 16168, Clearance Date 3/31/16. The U.S. Government is joint author of the work and has the right to use, modify, reproduce, release, perform, display, or disclose the work.

13. SUPPLEMENTARY NOTES
For presentation at 28th Annual Conference on Liquid Atomization and Spray Systems, ILASS-Americas 2016; Dearborn, MI May 15, 2016. Prepared in collaboration with Sierra Lobo , Inc.

14. ABSTRACT
Combustion instabilities can pose serious problems in the development of liquid rocket engines. In order to understand and predict them, it is necessary to understand how representative liquid rocket injector flames react to acoustic waves. In this study, a representative coaxial gaseous hydrogen / liquid oxygen (LOX) jet flame is visualized for both reacting and nonreacting cases. The jet flame was studied unforced, without acoustics, and forced, with transverse acoustic waves in a pressure node and a pressure antinode configuration. For unforced flames, reactions are found to cause a significantly more expanded plume due to the vaporization and expansion of the LOX. Flame holding is established at the lip with a particularly dominant LOX recirculation zone. Nonreacting convective structures propagate downstream at relatively constant velocity, while reacting structures start at a slow speed and gradually accelerate with downstream distance. These structures never reach the velocity of the nonreacting structures. Reactions shift the spectral content to lower frequencies, consistent with trends observed in the linear stability literature. For forced flames, acoustics do not appear to affect the flame holding. Dynamic mode decomposition detects jet response not only at the fundamental frequency but at higher harmonics as well. Reactions produce inconsistent trends in the harmonics: reactions promote harmonics at a pressure antinode while they damp harmonics at a pressure node.

15. SUBJECT TERMS
N/A

16. SECURITY CLASSIFICATION OF:			**17. LIMITATION OF ABSTRACT**	**18. NUMBER OF PAGES**	**19a. NAME OF RESPONSIBLE PERSON**
					D. Talley
a. REPORT	**b. ABSTRACT**	**c. THIS PAGE**	SAR	10	**19b. TELEPHONE NO** *(include area code)*
Unclassified	**Unclassified**	**Unclassified**			N/A

Standard Form 298 (Rev. 8-98)
Prescribed by ANSI Std. 239.18

ILASS Americas 28th Annual Conference on Liquid Atomization and Spray Systems, Dearborn, MI, May 2016

Acoustically Forced Coaxial Hydrogen / Liquid Oxygen Jet Flames

M. Roa* and D. Forliti[1]
Sierra Lobo, Inc.
Edwards, Ca 93524 USA

Al Badakhshan
ERC Inc.
Edwards AFB, CA 93524 USA

Doug Talley
Air Force Research Laboratory
Edwards AFB, CA 93524 USA

Abstract

Combustion instabilities can pose serious problems in the development of liquid rocket engines. In order to understand and predict them, it is necessary to understand how representative liquid rocket injector flames react to acoustic waves. In this study, a representative coaxial gaseous hydrogen / liquid oxygen (LOX) jet flame is visualized for both reacting and nonreacting cases. The jet flame was studied unforced, without acoustics, and forced, with transverse acoustic waves in a pressure node and a pressure antinode configuration. For unforced flames, reactions are found to cause a significantly more expanded plume due to the vaporization and expansion of the LOX. Flame holding is established at the lip with a particularly dominant LOX recirculation zone. Nonreacting convective structures propagate downstream at relatively constant velocity, while reacting structures start at a slow speed and gradually accelerate with downstream distance. These structures never reach the velocity of the nonreacting structures. Reactions shift the spectral content to lower frequencies, consistent with trends observed in the linear stability literature. For forced flames, acoustics do not appear to affect the flame holding. Dynamic mode decomposition detects jet response not only at the fundamental frequency but at higher harmonics as well. Reactions produce inconsistent trends in the harmonics: reactions promote harmonics at a pressure antinode while they damp harmonics at a pressure node.

*Corresponding author: Mario.roa.ctr@us.af.mil
[1]Now at University of St. Thomas, St. Paul, Minnesota

Introduction

Combustion instability associated with liquid rocket engines has been responsible for degradation of engine performance, increase in engine component stresses, and under extreme conditions, catastrophic engine failure. High-frequency instabilities, which are generally the most harmful in liquid rocket engines, can be driven when the disturbances associated with transverse acoustic resonances couple with the combustion process to form a feedback loop. In order to understand and predict combustion instabilities, it is necessary to understand how representative liquid rocket injector flames react to acoustic waves. In general, the thermoacoustic instability phenomenon is understood to be an interaction between acoustic waves and unsteady combustion. The unsteady heat release can amplify the acoustic field if the conditions are favorable. Due to the broadband nature of hydrodynamic instabilities, avoiding a detrimental coupling between acoustics and fluid dynamic mixing is challenging.

One way to try to mitigate the instabilities is to design an injector that does not couple with acoustic perturbation while it still provides the necessary mixing to sustain combustion. One such injector, used extensively for liquid rocket applications, is the shear coaxial injector [1-5]. In this injector configuration liquid oxidizer is injected surrounded by a gaseous fuel, as shown in Figure 1. The aerodynamic interactions at both fluid interfaces bring about hydrodynamic instabilities and atomize the liquid oxidizer into small droplets. These droplets evaporate and mix with the surrounding fuel and react.

There have been many models and efforts [6-9] to describe the atomization process with most being linear in nature and supported with empirical approximations to existing data. The models provide approximate liquid core lengths, time scales associated with growth rates of small disturbance, and droplet sizes and distributions. Due to the highly nonlinear nature of atomization, these models are limited in their range application and do not take reactions and the effects of high pressures into consideration. Accurate predictions of nonlinear, reacting high pressures atomization are left for intense computational studies.

In an effort to further understand high pressure atomization and combustion of a shear coaxial injector, experimental efforts have been carried at academic and national laboratories [10-12]. From these studies, there have been several proposed models of the breakup and dynamics of the liquid core of the shear coaxial injector under relevant rocket engine conditions. One such model is the classical phenomenological break up mod-

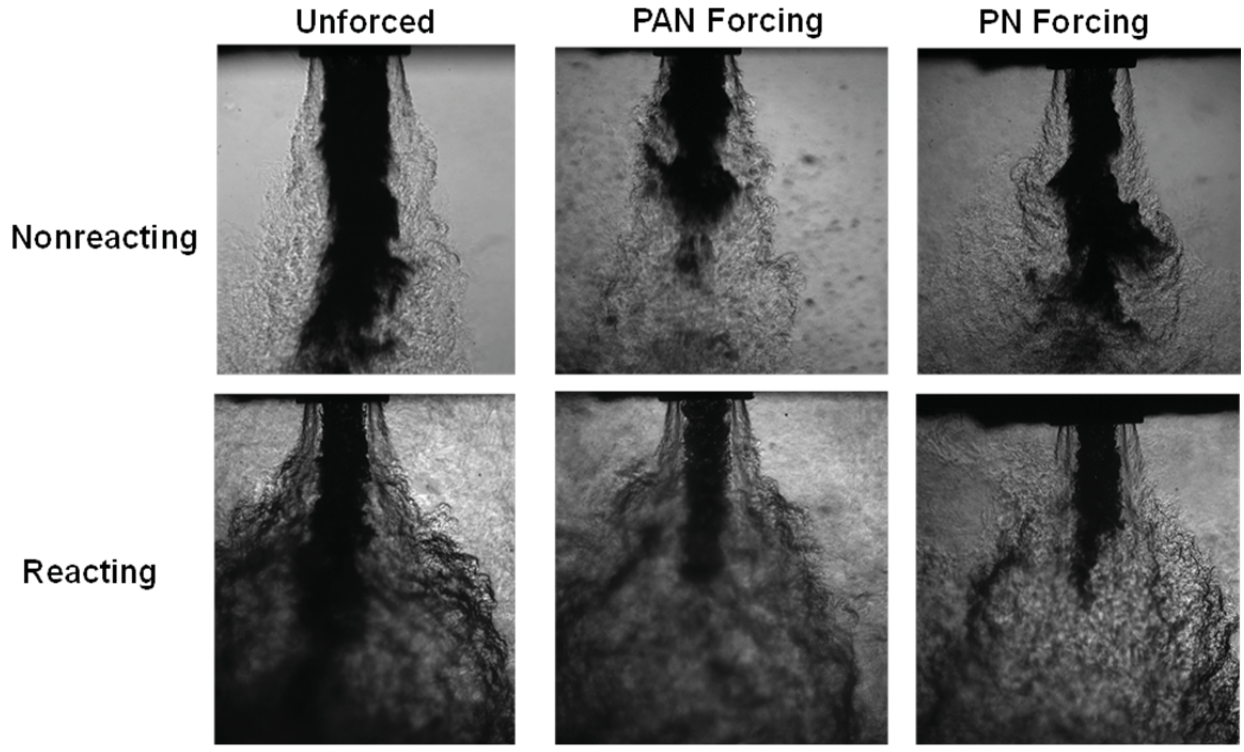

Figure 1. The shear coaxial flow of a LOX center surrounded by gaseous hydrogen. The first row shows the unreacting condition under same acoustic amplitude (0.34 bar) in a PAN and PN configuration. The second row shows the same conditions but reacting.

el by Reitz and Bracco [6]. In this model, the intact liquid core has ligaments and droplets continually shed due to surface instabilities, with the rate of liquid atomization dependent on momentum flux and velocity ratios between the liquid and the gas. This model has been typically used for rocket applications. Experimental and computational results have since raised questions of Reitz and Bracco model on its applicability to coaxial jets at rocket relevant conditions [13-15]. Another model is the core fragmentation model [16] where helical instabilities distort and breakup the liquid core. It is this helical mode that is responsible for some the large scale breakup of the LOX core observed for this investigation.

Since the LOX core has been observed to be the most prominent feature of shear coaxial injectors and with studies suggesting that combustion instabilities couple with LOX-post acoustics [17], an experimental effort was undertaken to study LOX core dynamics and breakup using a shear coaxial configuration subjected to high frequency acoustic forcing. A near field view at the injector exit was studied, limited to 6 LOX diameters, to capture the onset of the LOX core instabilities. The shear coaxial injector was studied both at reacting and nonreacting conditions. High frequency pressure anti-node (PAN) and a pressure node (PN) acoustic forcing was applied at the injector exit. Dynamic mode decomposition (DMD) was used to extract frequencies and spatial modal shape of the LOX response to the acoustic forcing under reacting and nonreacting conditions. There were differences in LOX core convective speeds and LOX core length between the reacting and nonreacting conditions for the acoustically unforced conditions. The LOX core behaved similarly under reacting and nonreacting conditions for the PAN acoustic forcing. A coupling of hydrogen (GH2) and LOX core shear layers occurred and a LOX core helical model was observed for the PN acoustic forcing for both reacting and nonreacting cases.

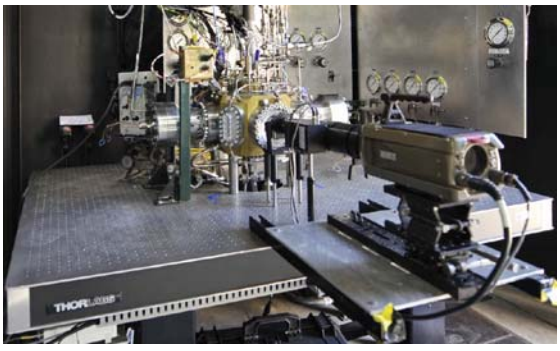

Figure 2. The experimental chamber and high speed camera.

Experimental Setup and Conditions

The experimental facility at the Air Force Research Laboratory (AFRL) at Edwards Air Force Base was used to investigate the coupling of transverse acoustic resonances with a single, shear coaxial, LOX/GH2 flow with varying acoustic perturbation amplitudes. Figure 2 shows the experimental chamber. The features of this facility were documented by Wegener et al. [12]. The injector geometry was the same as studied by Wegener et al [12]. Experiments were done at a mean chamber pressure of 34.45 bars (500 Psia). Nominal flow rates of liquid oxygen and hydrogen were 4.2 and 0.7 g/s, respectively, with a jet momentum ratio (GH2 to LOX) of 2.2. Both fluids had a Reynolds number on the order of 10^4. The LOX core had a Weber number on the order of 10^4. The LOX core was kept at constant temperature of 140 K and the GH2 at 250 K. The transverse acoustic resonance was induced through the use of carefully-controlled piezo-sirens, allowing excitation across a range of pressure amplitudes for discrete resonant chamber frequencies. The amplitude of the acoustic perturbations was varied incrementally from 0 bar (i.e. no acoustic forcing) to 0.34 bar (5 Psi). The pressure fluctuations were measured via Kulite high-speed pressure transducers (model XCL -100) located at different transverse locations, including the middle of the chamber which is the location of the injector. The mode shape of the acoustic field was altered through the phase relationship between the two acoustic drivers. The control of the mode shape allows for the PAN and PN regions of the acoustic mode to be placed at the exit of the injector. Resonant chamber frequencies of 3060Hz for PAN forcing and 2890 Hz for PN were selected. Previous studies on nonreacting experiments have shown a dramatic difference in the coupling mechanism depending on the local acoustic environment [18].

Shadowgraphy was selected as the basis of flow visualization due to the focus on the LOX core dynamic response to the acoustics, while providing an indirect view of the flame through the locations of density variations. A collimated light source and Vision Research v710 Phantom camera were used to acquire the high-speed shadowgraph images. The images were acquired at a 25 kHz frame rate with an exposure of 5 microseconds. The high-speed shadowgraph images were then analyzed using dynamic mode decomposition (DMD), similar to that described by Schmid [19], to identify when and how the LOX core and its shear flow responded to acoustic perturbations with and without heat release.

Results

Figure 1 shows instantaneous shadowgraph images of unforced and acoustically-forced cases under both unreacting and reacting conditions. The presence of the

flame has a dramatic effect on the topology of the LOX surface. For nonreacting, unforced conditions, the interface is highly blurred and appears to be in a fibrous atomization regime, consistent with Farago and Chigier [20] diagram of fiber type of atomization for the given Reynolds and Weber numbers. Evidence of large scale breakup of the LOX core length for the nonreacting and unforced condition, shown on the upper left in Figure 1, is evident 6 diameters away from the exit. Although the breakup is evident, a frequency cannot be determined nor a breakup length since the core extended beyond 6 diameters for the majority of shadowgraph images collected.

The shape of the acoustic forcing is shown in figure 3, with PAN forcing having the maximum pressure oscillations and the PN having the maximum velocity oscillations. For the acoustic forcing conditions, the same blurred and fibrous atomization was observed for both the PAN and PN conditions at the LOX shear layer, but a dramatic reduction of the LOX core length was observed, as shown in Figure 1. Massflow variations were observed of the LOX core subjected to PAN forcing. PN forcing resulted in a helical mode of the LOX core. For the PAN condition, the massflow variations are due to the increase and decrease of back pressure the injector experiences. In the PAN forcing, the shear coaxial flow is subjected to large pressure fluctuations. Using a simple Bernoulli argument, as the back pressure raises there is reduction in mass flowrate out of the injector and as the pressure dips an increase in LOX flowrate is achieved. These pressure fluctuations results in periodic surges of LOX mass flowrates, with large intact LOX fragments shedding away from the main core at the same acoustic forcing of 3060 Hz. For the PN condition the velocity perturbations are at their maximum. These velocity perturbations impart a helical movement on the LOX core given by the wavy or snake-like pattern of the LOX core. This wavy pattern has been reported previously by Boniface et al [10] and Woodward et al [21]. It is this instability that is responsive for the breakup of the LOX core closer to the nozzle exit under PN forcing compared to the acoustically unforced condition.

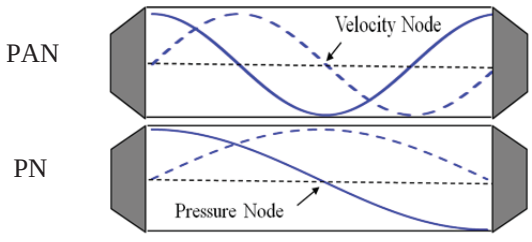

Figure 3. An instant in time of PAN and PN forcing. The solid line is the pressure fluctuations and the dash line is the velocity fluctuations. In PAN forcing, the injector experiences maximum and minimum pressure fluctuations. In PN forcing, the velocity fluctuations are maximum.

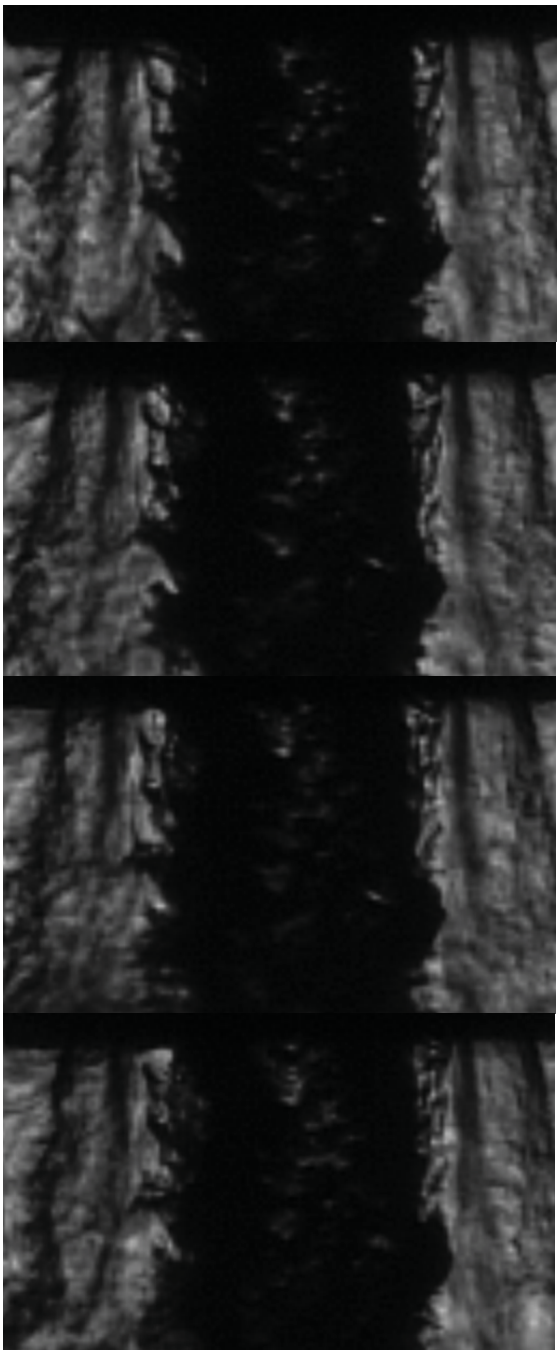

Figure 4. Sequential shadowgraph images demonstrating ligaments being shed off the LOX core for reacting cases. The time step between each image is 0.04 ms.

For the reacting conditions the presence of the flame results in a dramatic reduction in the fibrous nature of the surface, as expected, due to evaporation pro-

cesses as shown in closed up images in figure 4. The presence of the flame also shortens the length of the LOX core, which is again driven in part by the enhanced vaporization regardless of the acoustic forcing. Similarly, an expanded plume exists downstream due to the vaporization and expansion of the LOX, as shown in Figure 1. In the reacting flow cases, small ligaments were observed to be shed off the LOX core near the exit. These small ligaments are then entrained into a recirculation zone established below the LOX post. The ligament shedding close to the nozzle exit can be observed in figure 4, where the sequential images show ligaments on the either side of the LOX core being shed off. These ligaments get entrained into the LOX post recirculation zone if they are shed off within one LOX diameter. If shed past one LOX diameter, the ligaments convect with the rest of the LOX core. Figure 4 also shows an attached flame to inner lip of the GH2 exit.

No local flame extinction was observed regardless of the acoustic forcing amplitude. It has been experimentally observed when the strain rates associated with acoustic forcing is high enough [22], local extinction of the flame and the flame holding regions can occur. The extinction and re-ignition of the flame produces a flow field with uneven heat release that can couple with acoustic forcing, leading to a combustion instability limit cycle. Flame extinction and re-ignition events were not observed for any of the acoustic forcing conditions.

By extracting a column of pixels at each time step along the shear layer edge, dark streaks lines with constant slope represent convecting liquid structures can been seen in figure 5. These dark streaks, which are LOX core structures were observed to be traveling at constant velocity. For the unreacting case with no acoustic forcing, the shear layer between the LOX and the GH2 was approximate to Dimotakis [23] shear layer velocity. In the reacting condition, the shear layer velocity is not constant. Since the flame is attached to inner lip of the GH2 exit, there is a reduction in density between the interface between the LOX core and GH2. This reduced density pulls less on the LOX core, thus

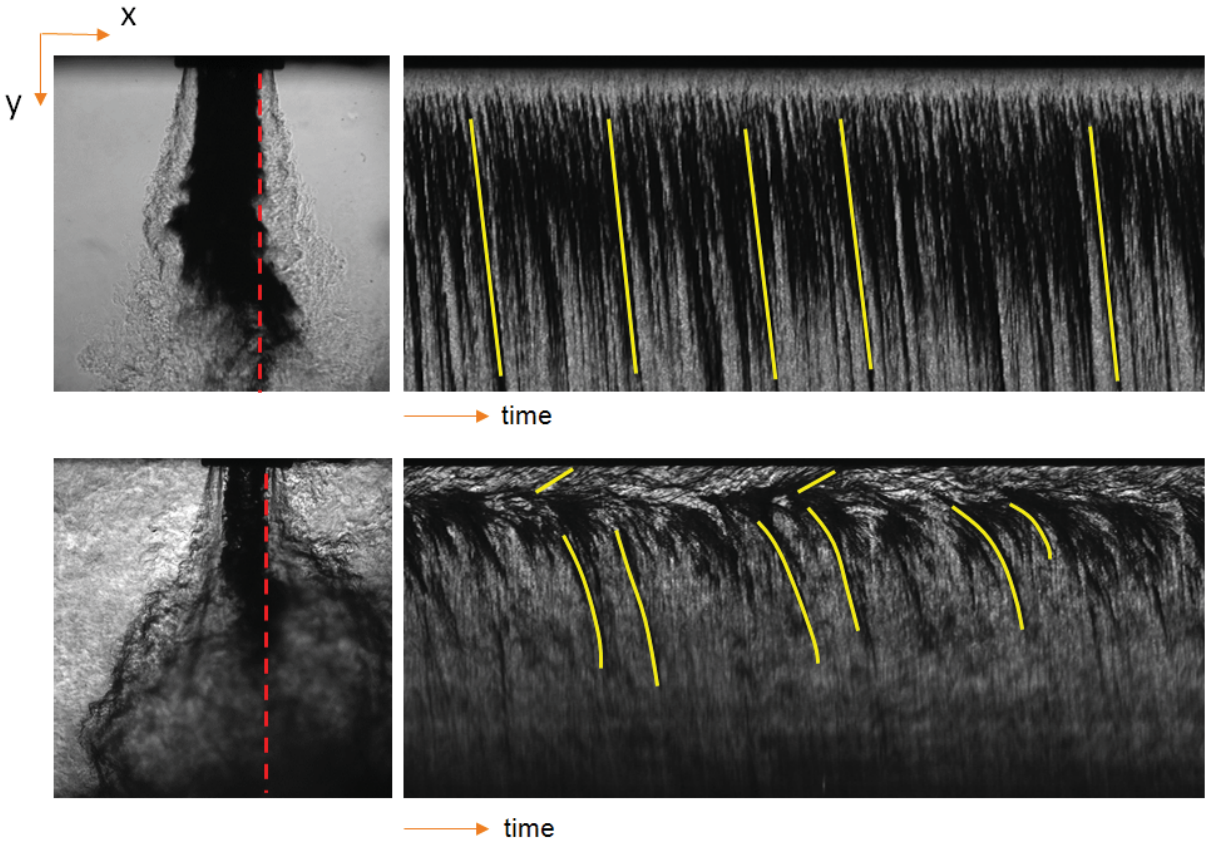

Figure 3. Extracted column of pixels at each time step along shear layer edge as a function of time. The dark streaks, traced with yellow lines, represent convecting liquid structures. The top is the unreacting condition and the bottom is the reacting condition. LOX core structures convect at a constant velocity for the nonreacting, acoustically unforced case. For the reacting condition, the LOX core exits at a low velocity and accelerates after one LOX core diameter away from the exit. The shear layer for the reacting condition never attains the same velocity as the unreacted condition.

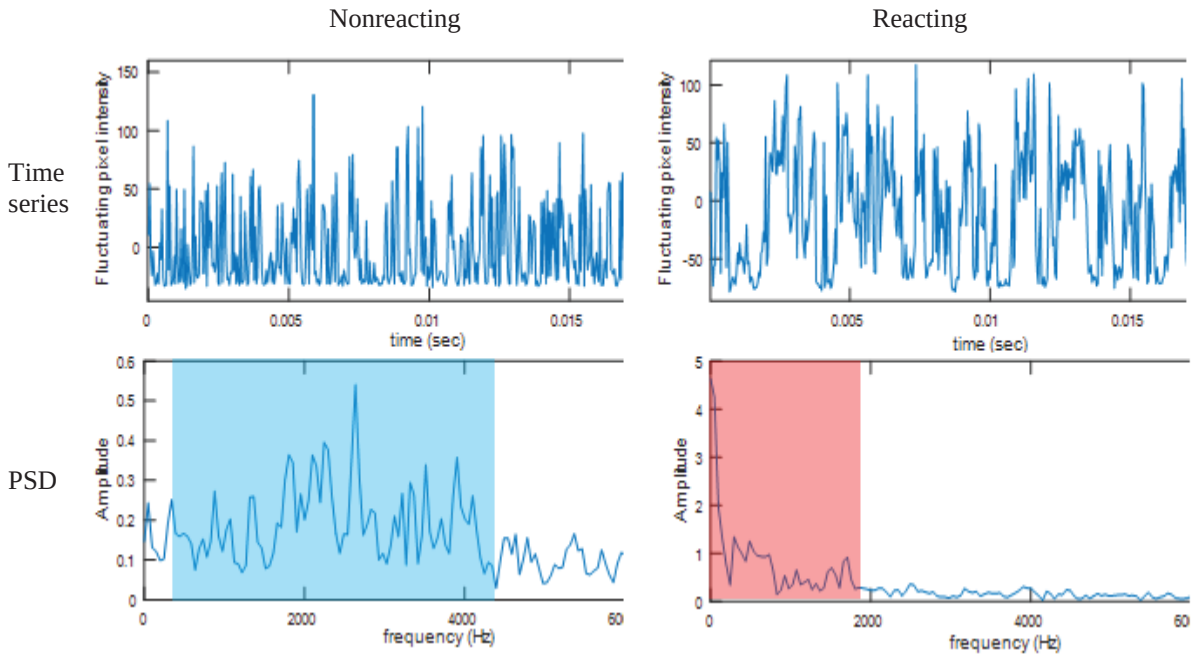

Figure 4. The pixel intensity of a pixel 2 diameters away from the exit along the shear layer, with its corresponding PSD. There is general shift to lower frequencies when the flame is present, consist with linear stability theory.

effectively convects slower compared to the nonreacting LOX core. Beyond the first diameter though, the LOX core starts to accelerate, as shown in figure 5 with the curved dark streaks, but never achieves the same convective velocity as the nonreacting condition. When the acoustic forcing was present the LOX core shape was too distorted to extract velocity information. Figure 5 also shows streaks with opposite flow orientation, illustrating the recirculation of the ligaments that were shed off within the first diameter as demonstrated in figure 4.

Although the trend in spectral content is highly dependent on the specific velocity and heat release profile, the presence of a flame is, in general, expected to result in a stabilizing effect and a shift to lower frequencies (e.g. Mahalingam et al. [24]). Spectral analysis of the measured intensity fluctuations in the near field of the inner shear layer (between the LOX core and GH2) shows there is a general shift of spectral content to lower frequencies when the flame is present. By analyzing the intensity fluctuations at a point 2 diameters away from the nozzle exit along the shear layer and performing a power spectral density, the general shift towards lower spectral content is observed, as shown in figure 6.

Dynamic mode decomposition (DMD) was used to identify the spectral content of both the forced and unforced cases. For the nonreacting case without acoustic perturbations, good agreement was found between the frequency associated with a convective mode and established scaling laws for shear coaxial jets [25]. For the

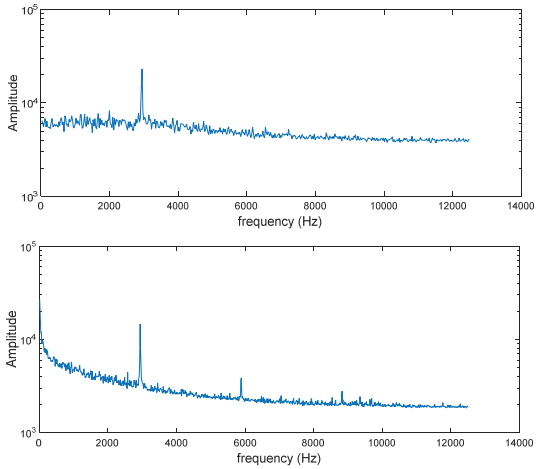

Figure 5. The DMD spectrum for the PAN nonreacting (top) and reacting (bottom) conditions. For the reacting condition, higher harmonics are present in the DMD analysis.

reacting condition without acoustic perturbations, there was no significant dominant mode, although a weak coupling between the inner and outer shear layers was observed at high frequencies.

Figure 7 shows the DMD spectrum for the maximum amplitude forcing condition with the injector placed at the PAN. It is evident from the DMD analysis that physical flow is coupled with the acoustic perturbation at the same driving frequency of 3060Hz. The case shown in figure 7 is for both reacting and nonreacting

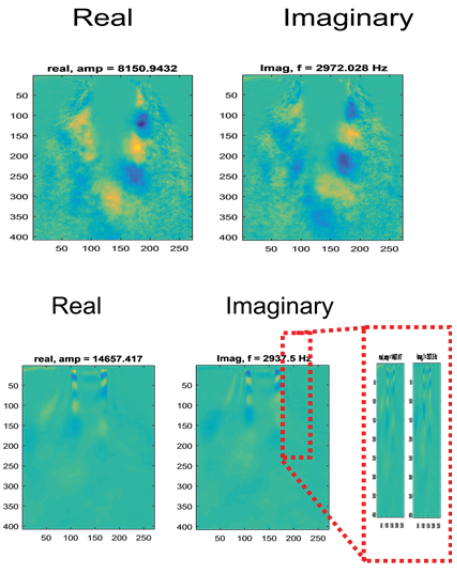

Figure 9. The DMD shape mode of the PAN unreacting (top) and reacting (bottom) condition.

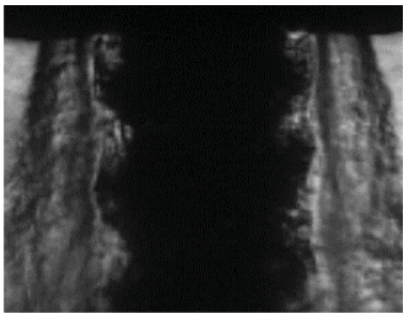

Figure 10. Organized motion of the LOX core under PAN perturbations and reacting.

conditions. The peak-to-peak pressure amplitude for this case was approximately 0.36 bar (5.3 psi). For the reacting condition there is a clear indication of coupling between the acoustics and the inner shear layer instability, including coupling at higher harmonic frequencies, but this coupling is not evident in the nonreacting case. Figure 8 shows the DMD spatial modes. The DMD spatial mode illustrates a symmetric shear layer response of the LOX core, as indicated by the axially aligned positive (yellow) and negative (blue) intensity fluctuations in the DMD spatial mode shapes. This symmetry is expected as the mechanism that is associated with PAN forcing relates to azimuthally-coherent mass flow fluctuations in the LOX core flow as discussed earlier. Although the LOX core response is symmetric, the scales of the axisymmetric structures are not the same. For the reacting case these structures are smaller compared to the nonreacting condition shown in Figure 1. Figure 10 shows a shadowgraph image of

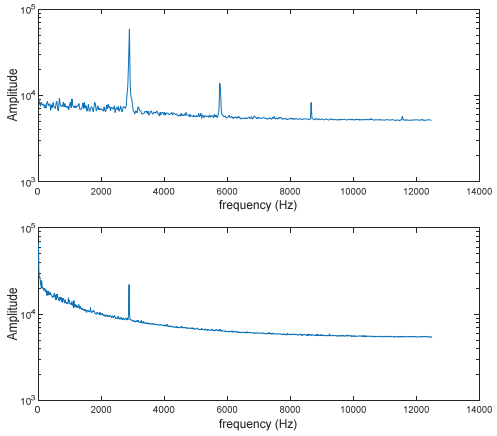

Figure 11. The DMD spectrum for the PN nonreacting (top)and reacting conditions (bottom). For the unreacting condition, higher harmonics are present in the DMD analysis.

the injector near field, and a vertical row of shear layer structures can be seen at the LOX core boundary. These structures are thought to be smaller because the LOX core velocity is slower compared to the nonreacting case, resulting in reduced massflow variations. The LOX core also experiences roll-up motion that is in the opposite direction then would be expected based on the presence of the high-speed GH2 flow. The LOX core rollup travels upstream, opposite of the both the GH2 and LOX core flow, into the wake and recirculation region underneath the LOX post. The observed vorticity orientation suggests the inner shear layer is interacting with the LOX post's low-speed wake region. The combination of the reduced interfacial density, as discussed earlier, and the low-speed wake region effectively slows the LOX core resulting in a decrease in massflow variations subjected PAN forcing. The PAN interactions are first detected when the acoustic perturbation amplitude is approximately 0.13 bar (2 psi). The coherent organized motion, shown in figure 10, at the surface of the LOX core is also first observed at this amplitude.

Figure 11 shows the DMD spectrum for the maximum forcing amplitude PN forcing, similar to figure 7. Similar to the PAN condition, a coupling of the shear layers at a frequency of 2890 Hz was observed for the PN acoustic forcing. There is a reversal of the harmonics detected for the nonreacting and reacting conditions. For the nonreacting condition subjected to PN forcing higher harmonics are detected. The higher harmonics are dampen for the reacting condition. This results is opposite of the PAN results. Figure 12 shows the DMD spatial modes associated with the peak frequencies in figure 11. In the figure 12, the large alternating blue and yellow pattern shows a helical mode excitation of the LOX core when perturbed by PN forcing. A coupling between the inner and outer shear layers, as observed

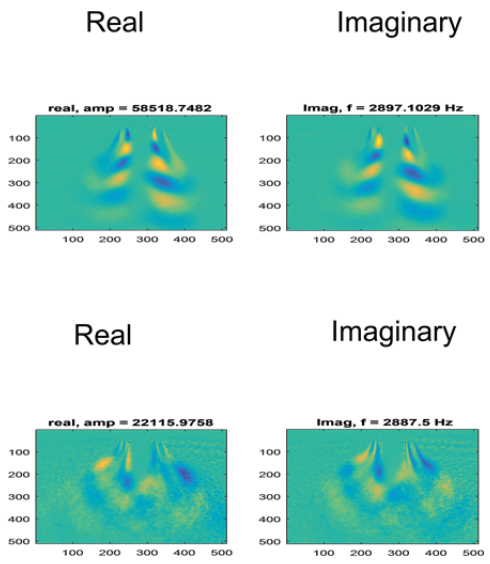

Figure 12. The DMD shape mode of the PN nonreacting (top) and reacting (bottom) condition.

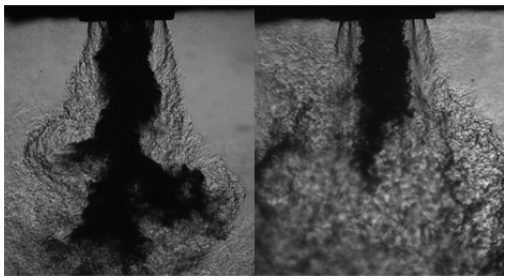

Figure 13. Full field images of the nonreacting (left) and reacting (right) PN forced condition. For the reacting condition there is very little LOX core motion.

by Dahm et al [26], is present when the flow is unreacting, with the LOX core shear layer dominating. The slim alternating blue and yellow streaks to either side of the LOX core illustrate the coupling of GH2 shear layer to the LOX core shear layer. This coupling between the inner and outer shear layer was not observed for PAN conditions when no reaction was present. A coupling was observed when a flame was present. For the reacting condition, an anti-symmetric structure with coherent coupling between the outer and inner shear layers was present.

Figure 13 shows side by side images of the nonreacing and reacting PN forced conditions. For the nonreacting condition, the LOX core responses dramatically to the PN forcing and a helical mode is observed in figure 13. For the reacting condition, the LOX core is slow to respond to the PN forcing. It was observed that GH2 shear layer was in phase with acoustic forcing and LOX core was out of phase with the respect to the incoming acoustic wave. From figure 13 the helical shape of the nonreacting LOX core begins close to the nozzle exit, unlike reacting condition where helical turning starts further away from the nozzle exit compared to nonreacting case. It is believed that the anchored flame at the exit of the nozzle dampens the velocity perturbation at the nozzle exit for the PN forcing, but not for the pressure perturbations in the PAN conditions. The higher harmonics are believed to be dampen because of the LOX core delayed reaction to PN perturbations and the helical shape is not as pronounced under reacting conditions.

Conclusion

The near field of shear LOX/GH2 coaxial flow was investigated under relevant rocket conditions; both reacting and nonreacting conditions were subjected to acoustic forcing. Under reacting conditions, the rapid expansion and vaporization of the LOX core caused an expanded plume that was presented for all acoustic forcing conditions. A LOX recirculation zone was present downstream of the LOX post. In the reacting condition, ligaments where shed off from the LOX core and entrained into the LOX post recirculation zone. Flame holding was established at the inner lip of the GH2 exit. Convective velocities of the LOX core were constant under nonreacting conditions but not in the reacting conditions, where the flow started at a slow speed and gradually accelerated. A shift of spectral content to lower frequencies occurred when a flame was present.

Dynamic mode decomposition captured the physical response of the LOX core under different acoustic forcing. For PAN forcing the LOX core experienced variations of the mass flowrates for both nonreacting and reacting conditions, but the liquid structures differed greatly in size. For PN forcing the nonreating case, a LOX core helical mode was present and the inner outer shear layer coupled together. For the reacting case, the LOX core response was out of phase with respect to the acoustic forcing. Given the physical differences and responses of the nonreacting flows compared to the reacting flows to low amplitude, high frequency acoustic perturbation, it is vital these differences be understood to better control combustion instabilities.

Nomenclature

DMD	Dynamic mode decomposition
GH2	Gaseous Hydrogen
LOX	Liquid Oxygen
PAN	Pressure Anti-node
PN	Pressure Node

Acknowledgements

This work was funded by Airforce Office of Scientific Research.

References

1. Juniper, M.P., and Candel, S.M., *Journal of Fluid Mechanics* 482:257-269 (2003)
2. Hakim, L., Schmitt, T., Ducruix, S., and Candel, S., *Combustion and Flame* 162:3482-3502 (2015)
3. Ibraim, E.A., Kenny, R.J., and Walker, N.B., 42nd *AIAA/ASME/SAE/ASEE/ Joint Propulsion Conference*, Sacramento, Ca, USA, July 2006
4. Puissant, C., and Glogowski, M.J., *Atomization and Sprays* 7:467-478 (1997)
5. Yang, V., and Anderson, W., *Liquid Rocket Engine Combustion Instability*, American Institute of Aeronautics and Astronautics, Inc. 1995, p. 46.
6. Reitz, R.D., and Bracco, F. V., *Physics of Fluids* 25:1730-1742 (1982)
7. Lin, S.P., and Lian, Z.W., *AIAA Journal* 28:120-126 (1990)
8. Mohanta, L., Cheung, F., and Bajorek, S.M., *Physica A*443:333-346 (2016)
9. Lin, S.P., and Ibrahim, E.A., *Journal of Fluid Mechanics* 218:641-658 (1990)
10. Boniface, Y., Reeb, A., Woodard, R., Pal, S., and Santoro, R. J., *Proceedings of the 11th Annual PERC Symposium on Propulsion*,University Park, PA, USA, November 1999,. pp 110-119
11. Pal, S., Moser, M.D., Ryan, H.M., Foust, M.J., and Santoro, R.J., *Atomization and Sprays* 6:227-244 (1996)
12. Wegener, J.L., Leyva, I.A., Forliti, D.J., and Talley, D.G., *52nd AIAA Aerospace Sciences Meeting*, National Harbor, MD, USA, January 2014
13. Oefelein, J.C., and Yang, V., *Journal of Propulsion and Power*, (14): 843-857 (1998)
14. Yang, V., *Symposium (International) on Combustion*, (28) :925-941 (2000)
15. Zong, N., and Yang, V., C*ombustion Science and Technology*, (178): 193-227 (2006)
16. Andrews, M. J., *Atomization and Sprays* 3:29-54 (1993)
17. Locke, J.M., Pal, S, Woodard, R.D., and Santoro R.J, 46th *AIAA/ASME/SAE/ASEE/ Joint Propulsion Conference*, Nashville, TN, USA, July 2010
18. Forliti, D.J., Badakhshan, A., Wegener, J.L., Leyva, I.A., and Talley, D.G *53rd AIAA Aerospace Sciences Meeting*, Kissimmee, FL, USA January 2015.
19. Schmid, P. J., *Journal of Fluid Mechanics* (656):5-28 (2010)
20. Farago, Z., and Chigier, N., *Atomization and Sprays* 2:137-153 (1992)
21. Woodard, R.D, Pal, S., Farhangi, S., and Santoro, R.J., 42nd *AIAA/ASME/SAE/ASEE/ Joint Propulsion Conference*, Reno, NV, USA, January 2001
22. Chaouki, G, Smith, O. I., and Karagozain, A. R,. 39th *AIAA Aerospace Science Meeting S*acramento, Ca, USA, July 2006
23. Dimotakis, P.E., *Am. Inst. Aeronaut. Astronaut. J.* 24(11):1791-1796
24. Mahalingam, S., Cantwell, B.J. and Ferziger. J.H., *Physics of Fluids A: Fluid Dynamics* (3):1533-1543 (1991)
25. Schumaker, S, A., *An experimental investigation of reacting and nonreacting coaxial jet mixing in laboratory rocket engine*, Thesis, (2009)
26. Dahm, W.J.A, Frieler, C.E. and Tryggvason, G., *J. Fluid Mech*.(241):371-402 (1992)